UNIVERSITY OF STAVANGER

A computational model of DOPA regulation, dopamine synthesis in the presynaptic neuron, and release into the synaptic cleft

by

Pegah Tajeddini

Master Thesis in Biological Chemistry

submitted to the
Faculty of Science and Technology
Department of Biology, Chemistry and Environmental Engineering

June 2022

UNIVERSITY OF STAVANGER

Abstract

Faculty of Science and Technology
Department of Biology, Chemistry and Environmental Engineering

Master Thesis in Biological Chemistry

by Pegah Tajeddini

Background: Neurotransmitters and the way neurons communicate with each other have received a lot of attention in recent decades. Dopamine is one of the most important neurotransmitters. Unbalanced levels of dopamine can be associated with physical and psychological disorders like Parkinson's disease, schizophrenia and addiction[1]. This study shows different regulations performing in the presynaptic neuron to maintain balanced DA levels and DOPA as its precursor.

Methods: Fortran subroutine LSODE were used to solve rate equations and model the assumed controlling system to find the relationship between molecules and enzymes contributing in this system.

Results:This study shows that in the presence of different perturbation or even treatments, DOPA is the controlled variable and dopamine as controlling variable try to help DOPA maintain in homeostasis. In the studying of dopamine release into the synaptic cleft, the calculation suggested hysteretic behaviour.

Conclusion:There should be a meaningful relationship between varied levels of dopamine and steady state conditions of DOPA in presence of different perturbation and varied amount of enzymes. The controller system should help homeostasis of DOPA and dopamine in presynaptic neurons, and robust response to significant signals like action potential.

Acknowledgements

I would like to express my deepest thanks to my supervisor Professor Peter Ruoff, for his outstanding support from the start day of my master studies to the end.
I did not choose computational neurobiology because I was expert in it, instead, because I did not have any experience in it, and it was always a question on my mind: "in what way programming can help biology?" I decided to fight one of my biggest fears, and there was no one could help me better than you Peter, in this challenge.

I would also pay my regards to my friend and coach, Dr Nader Marzban, who inspired me to start this journey, always guided me and I learned from him a lot in neuroscience.

Finally, I give my very special thanks to my husband for his care and support during this year. He is a light in the darkest moments, the best friend in hardest situations and a reason to continue the best way that I can.
Pegah Tajeddini
Stavanger, June 15, 2022

...

Contents

List of Figures

Abbreviations

AADC	**A**romatic **A**mino-acid **D**ecarboxylase
ADHD	**A**ttention **D**eficit **H**yper **A**ctivity
DA	**D**opamine
DAT	**DA T**ransporter
DOPA	**D**ihydr**O**oxy **P**henyl **A**alanine
HVA	**H**omo**V**anillic**A**cid
MAO	**M**ono **A**mine **O**xydase
PD	**P**arkinson's **D**isease
ROS	**R**eactive **O**xygen **S**pecies
TH	**T**yrosine **H**ydroxylase
Tyr	**Tyr**osine
TYR	**TYR**osinase
VMAT	**V**esicular **M**ono**A**mine **T**ransporter

Dedicated to my parents, and my brother Pedram, who are always in my heart despite the distance
and Hooman, for his unconditional care and support...

Chapter 1

Introduction

1.1 Nervous system

The human nervous system is a very complex network of many single cells called neuron. In this system, there are also other cells than neurons, which are very important in supporting neurons, called glial cells (glia). To describe more a typical nerve cell (neuron) morphologically, we can mention 4 regions of a single cell named cell body, dendrite, axon, and presynaptic terminal [5].

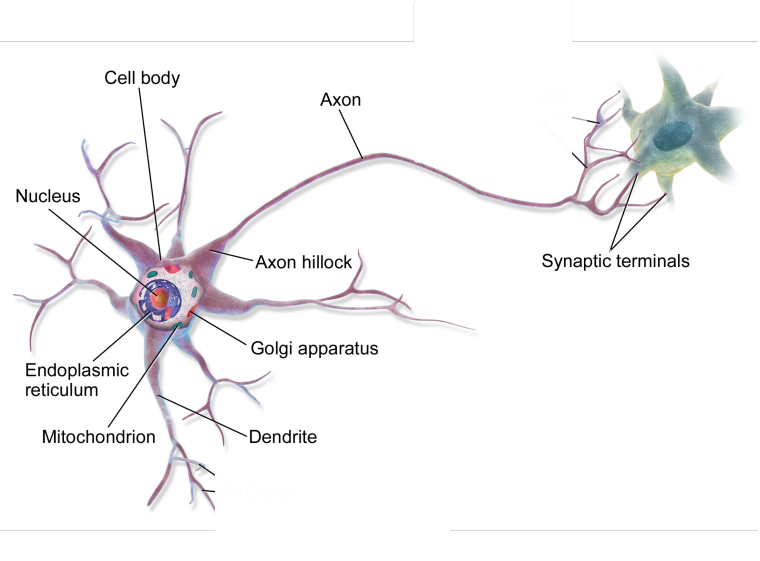

FIGURE 1.1: Single neuron [2]. Typical neuron is made up of 4 main parts of dendrite, axon, cell body, and the presynaptic terminal.

Signal transmission is a very important feature of the nervous system in transferring data from one neuron to the other and along each neuron. This signalling is performed

via ion -flow across cell membrane and electrical conducting of the nerve cell. The nerve cells are not physically connected to each other but communicate through synapses. Synapse is where a neuron is in contact (not physically) with another neuron or cell. A cell that transmits signals from its swollen terminal called presynaptic neuron and a signal receiving cell called postsynaptic cell. There are two types of synapses in the nervous system: electrical and chemical. We more focus on chemical synapses here [5]. Neurons form a wide signalling network and communicate through it. Principle of this signalling is almost the same in every neuron. To produce a behaviour, four types of signal contribute: input signal, trigger signal, conducting signal and output signal. This signalling can be determined by electrical properties of nerve membrane. The resting membrane potential is between -40 to -80mV (-65mV in general). The nerve cell has the excess of the negative charge inside and excess of positive outside. This electrical charge is made by inflow and outflow of ions, especially Na^+ and K^+. We consider the outer charge as zero, so the overall potential is negative at the rest. After the action potential stimulus, membrane voltage raise to +40mV because of inflow of cations to cell [5].

$$V_m = V_{\text{in}} - V_{\text{out}} \tag{1.1}$$

Less negative membrane potential, is called depolarization. When depolarization reaches a critical level, named threshold, voltage gated channels open and lead to produce an all-or-non action potential.

Ion channels in the nerve membrane, for example, K^+, Na^+ channels, have an important role in altering the nerve membrane potential according to rest status or action potential within the neuron. There are two types of ion channels: rest, and gated. Rest channels are always open and try to keep the membrane in the rest status. Gated channels are open by receiving action potential. Ca^{2+} channels control the influx of Ca^{2+} that alter many processes as well as neurotransmitter release to the synaptic cleft. Channels are modified and are affected by protein phosphorylation, ions that block the channels, toxin and poisons, and drugs. There are also antibodies, for example, in autoimmune diseases that can block the channels [5]. The role of Ca^{2+} influx through the channels will be discussed later in the introduction.

In the chemical synapses, signalling output is generated by neurotransmitter release. Neurotransmitters are molecules stored in special vesicles in the presynaptic nerve terminal. There are approximately 5000 of neurotransmitter molecules in each vesicle. After nerve depolarization, the vesicle fuse to the membrane by inflow of Ca^{2+} ions and release its contents by exocytosis. Neurotransmitters then, bind to the receptors in the postsynaptic neuron and based on the receptor, may activate or inhibit the postsynaptic neuron. This steps cause a delay as short as 0.3 ms at the chemical synapses and last for several milliseconds, so the chemical synapse does not have the speed of electrical synapses. Neurotransmitters also can be reuptaken by the presynaptic neuron or removed from the synaptic cleft by the enzymes. The synaptic vesicle that has been added to the terminal membrane, is retrieved and recycled to generate new synaptic vesicles [5].

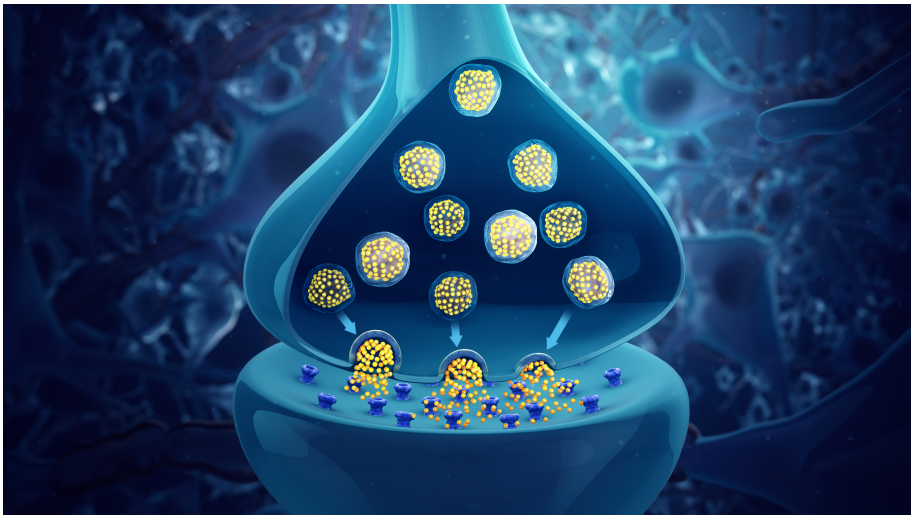

FIGURE 1.2: Neurotransmitter release into the synaptic cleft [3]. Neurones are not connected to each other physically. In chemical synapses, neurotransmitters are released from the presynaptic neuron and diffuse to the postsynaptic neuron.

As discussed earlier, transmission in the chemical synapses divides into four steps: transmitter synthesis, transmitter storage and release, transmitter interaction with the postsynaptic cell receptors and removal of neurotransmitter from the synaptic cleft. We can define neurotransmitter as substances released to the synapse and affect postsynaptic cell, which can be neuron, muscle or gland. Two classes of transmitters used for signalling in the nervous system: small-molecule transmitters and neuroactive peptides. Nine substances are generally accepted as small-molecule transmitter: acetylcholine, dopamine, norepinephrine, epinephrine, eerotonin, histamine, Y-aminobutyric acid, glycine and glutamate [5].

The neurotransmitter dopamine, nor-epinephrine and epinephrine are made from the amino-acid tyrosine by a common pathway. Enzymes tyrosine hydroxylase, aromatic

aminoacid decarboxylase, dopamine hydroxylase, pteridine reductase, and phenylethanolamine - N-methyl transferase are parts of this pathway [5].

1.2 Dopamine

Dopamine is a neurotransmitter produced by dopaminergic neurones in the central nervous system (CNS). 90% of the brain dopaminergic cells reside in the ventral part of mesencephalon. Mesencephalic dopaminergic system is divided into several nominal system and one of the best known is the nigrostriatal systems, originated from the zona compacta to dorsal striatum. This pathway is important in controlling voluntary movement. Dopaminergic cells in ventral compacta area are more important in emotion-based behaving such as reward and motivation [6].

During dopamine synthesis, the tyrosine is converted to L-dihydroxyphenylalanine (L-dopa) by enzyme tyrosine hydroxylase (TH). Tyrosine concentration varies based on the meals we eat, but it should not affect the dopamine synthesis [7]. The aromatic amino acid decarboxylase (AADC), also known as dopa decarboxylase (DDC), catalyzes the decarboxylation of L-dopa to dopamine. Free dopamine in the cytosol, is oxidised to aminochrome by tyrosinase or enzymes with peroxidase activity. Aminochrome is a precursor to neuromelanine, giving the dopaminergic neuron its dark colour. TH and AADC are associated with enzyme vesicular monoaminergic transporter-2 (VMAT-2), catalyzes dopamine uptake into monoaminergic synaptic vesicles to prevent dopamine being free in the cytosol . Cytosolic dopamine converts to homovanillic acid (HVA) by sequential reactions, where start by dopamine oxidative deamination catalyzed by monoamine oxidase (MAO)(which is placed in the outer membrane of mitochondria) or methylation by catechol ortho-methyl transferase (COMT) [8].

However dopamine has also a somatodendritic release, here we focus on axonal release. We assume that it is fast synaptic vesicle exocytosis. At fast synapses, SNARE complex is formed during fusion and its release is restricted to active zones close to voltage gated calcium channels. Upon depolarization of presynaptic plasma membrane by receiving action potential, Ca^{2+} enters to voltage-gated Ca^{2+} channels and triggers the fusion of vesicle and the membrane , so dopamine release [9].

There are two kinds of discharge activity in the dopaminergic neurons. Single spikes, at a mean frequency of 5Hz maintain the neuron and synapse in a normal conditions. 2-6 bursts of action potential with frequency of 15-30Hz, raise the DA levels in the synaptic cleft significantly [10].

A membrane transporter protein which seems to have negative feedback on dopamine release is DAT (DA transporter). In previous studies, it was shown that DAT is a transporter protein of nearby neurons which clears dopamine from the synaptic cleft by reuptaking it into the cytosol. It is an important way to inactivating DA in the synaptic cleft [11]. DA uptake by DAT is coupled with translocation of one Cl^- and two Na^+ ions. This translocation leads to more positive charge of the neuron and depolarization of the membrane, which may cause increased activation of D2 coupled with $G_{\alpha i}$ subunit of G -protein, and leads to reduction in vesicle fusion, and dopamin release [12].

There are G_i coupled D2 autoreceptors in the presynaptic neuron membrane which have negative feedback on dopamine synthesis by inhibiting of TH, enhancing dopamine uptake from the synaptic cleft with effects on dopamine packaging into vesicles by regulating VMAT2 [9]. Study by Best et.al [7] show that when firing of action potential continues for longer time at 15Hz, Tyrosine hydroxylase activity decrease by the feedback from DA autoreceptors . There are at least 5 dopamine receptors named D1 to D5. D4 is expressed in the limbic area and hypothalamus and mostly related to emotion responses [5].

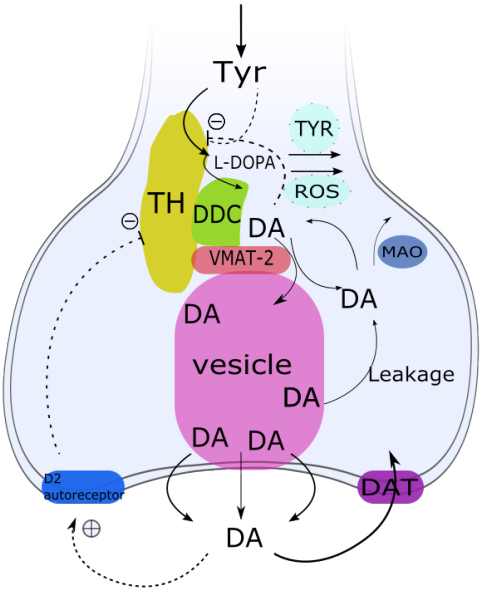

FIGURE 1.3: Regulation of DA synthesis. Enzymes TH, DDC and transporter protein VMAT2 form a complex leads to DA synthesis by a channeling mechanism. This mechanism is assumed to reduce the oxidation of dopamine by MAO and other oxidants. Dopamine is stored in vesicles until the action potential trigger the vesicle release of dopamine into the synaptic cleft.

Dopamine and its precursor DOPA are related to many diseases and addiction. Studies od patients also show a relationship between dopamine and schizophernia. Postmortem

studies have shown higher dopamine, HVA concentration and dopamine receptor density in the brain compared to the healthy subjects [13]. All molecular genetic studies of ADHD (attenntion-deficit hyperactivity disorder) showed significant association of genes for dopamine D4 and D5 receptors, also serotonin and dopamine transporter (DAT) [14]. To mention some examples of dopamine relation to addiction, we can refer to inhibitory role of cocaine on DAT [11], also long term decrease in expression of D2 in alcohol consumers. Another example can be the increase of dopamine levels by cigarette smoking, and producing substances inhibiting MAO [15]. PD is a common neurodegenerative disease related to low amounts of dopamine. PD affects 1-3% of people older than 80 years. Presence of Lewy bodies and degeneration of dopaminergic neurons are characteristics of PD. There is a relationship between DAT reduction and PD. PD's clinical symptoms are rigidity, tremor and postural instability. Response to Levodopa therapy is favourable in this disease [16]

Current drug for treatment of PD and other diseases related to dopamine deficiency, is Levodopa (DOPA). Levodopa (DOPA) is a natural amino acid absorbed in the small intestine and goes to the brain by passing blood-brain barrier. To be able to pass this barrier it breaks down, and only a small part of it can enter the brain. There, enzyme L-amino acid decarboxylase AAAC catalyses the decarboxylation of this molecule and form dopamine [17]. In our model in this study, Levodopa treatment is shown as k_{22} which will be discussed later in the Results and Discussion.

DOPA should be stable near its set point for the best performance which called homeostasis. To maintain this value, there are some controlling systems helping dopamine levels adapt in presence of different perturbation. There are many regulatory interactions in dopamine system and these reactions are not linear since many molecules are contributing in this process.

1.3 Homeostasis and controller systems

To introduce the word "homeostasis", first, Walter Cannon described it as "mechanisms performed to keep organisms in the steady state with very narrow limits, condition very necessary to survive " [18]. The term "homeostasis" comes from the greek word meaning "steady and same". A good example of homeostasis is our body temperature control in different situations. For example, sweating in response to overheating which cools the body. On the other hand, reducing blood circulation to the skin in cold surroundings. This control is possible with positive and negative feedback loops. Positive feedback is a response by increasing the departure even more to reach the normal conditions.

Negative feedback (opposite feedback) try to keep the normal conditions by opposing environmental changes [19].

There are 16 types of two-component feedback controller motifs , dividing equally into negative and positive feedback loops [20]. Each of these groups divides in to 2 operation work models of inflow and outflow control. These motifs are to show how robust homeostasis is performed in the living cell. However, robust homeostasis is necessarily associated with zero-order flux conditions and not only feedback structures. One of the two substances present in each controlling motif is controlled variable, which should be near its set point or its homeostatic conditions, and the other component is the manipulated or controller variable, which changes its concentration to keep the controlled variable at its set point.

1.4 Integral control

Integral control is an engineering concept, first invented/used to the robust steering of ships. In integral control, the difference between concentration of a controlled variable and its set point (the "error") is integrated over time. The integrated error is proportional to the concentration of manipulated (controller) variable, which oppose perturbations and thereby keeps the controlled variable at its set point [21]. To perform integral control in biological systems, one approach is to remove the manipulated variable by zero-order kinetics [20][1]. Autocatalystic formation or second order reaction are other kinetic forms to introduce integral control to biochemical systems [22][23]. Figure 1.4 shows an overview of four controller motifs. Controller motif 2 has been used in our model to describe DOPA/DA regulation.

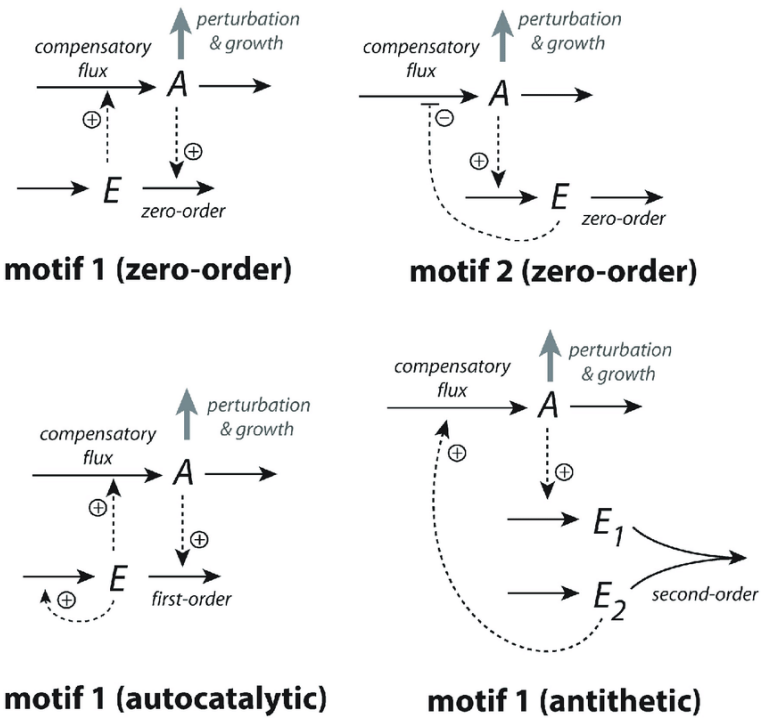

FIGURE 1.4: Controller motifs[4]. The most promising controller is motif 2 zero-order controller working based on derepression. Controller motif 1 shown here works based on autocatalysis, and antithetic motif is a new discovered controlling system. This study is based on motif 2 zero-order controller.

The principle of integral control can be viewed as follows:

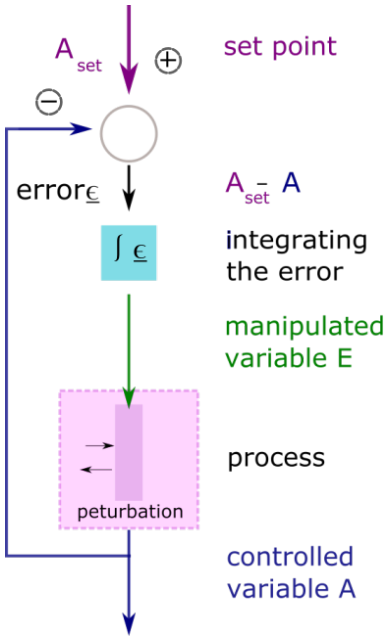

FIGURE 1.5: The principle of negative feedback regulation and integral control. Variable A remains in its set point A_{set} by integrating the error ϵ in time. Manipulated variable E opposes the perturbation, thereby keeping A at its set-point A_{set}.

In the following figure we can see a simple model of negative feedback controller system, which can be considered as TH inhibition by dopamine where P represents Tyr, A is DOPA and E is dopamine.

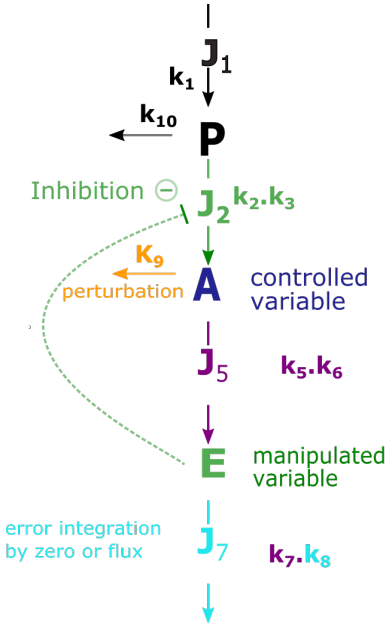

FIGURE 1.6: Negative feedback regulation and integral control in simple model of TH-DA regulation. Pairs of k_i , k_j repectively represents V_{max}, K_M. By increasing perturbation (k_9, j_7 increases with zero-order flux, resulting in the decrease of the manipulated variable E. This leads to a decrease in inhibition ("derepression") and an increase of the controlled variable A. This controller system continues working with raise in perturbation until controller variable E goes to zero and the system breaks down.

Equations 1.2 to 1.13 show how the controller works.

$$\frac{dP}{dt} = k_1 - \left(\frac{k_2 \cdot P}{k_3 + P}\right) \cdot \left(\frac{k_4}{k_4 + E}\right) - k_{10} \cdot P \tag{1.2}$$

$$\frac{dA}{dt} = \left(\frac{k_2 \cdot P}{k_3 + P}\right) \cdot \left(\frac{k_4}{k_4 + E}\right) - k_9 \cdot A - \left(\frac{k_5 \cdot A}{k_6 + A}\right) \tag{1.3}$$

$$\frac{dE}{dt} = \left(\frac{k_5 \cdot A}{k_6 + A}\right) - \left(\frac{k_7 \cdot E}{k_8 + E}\right) \tag{1.4}$$

In zero-order conditions, K_M in removal of E (DA) is much lower than E, and we can consider it close to 0, so in the equation, we can assume that the second part is equal to k_7(E/(k_8+E) ≈1. Further rate equations are as below:

$$if \quad \frac{dE}{dt} = \left(\frac{k_5 \cdot A}{k_6 + A}\right) - k_7 = 0 \quad \Rightarrow \quad A_{ss} = A_{set} = \frac{k_6 k_7}{k_5 - k_7} \tag{1.5}$$

$$\dot{E} = \frac{k_5 \cdot A}{k_6 + A} - k_7 = \frac{k_5 \cdot A}{k_6 + A} - \frac{k_7 \left(k_6 + A\right)}{k_6 + A} = \frac{k_5 \cdot A - k_6 k_7 - k_7 \cdot A}{k_6 + A} \tag{1.6}$$

$$\frac{\dot{E}}{k_6 k_7} = \frac{\frac{(k_5 - k_7) \cdot A}{k_6 k_7} - 1}{k_6 + A} \tag{1.7}$$

$$A_{set} = \frac{k_6 k_7}{k_5 - k_7} \tag{1.8}$$

$$\frac{\dot{E}}{k_5 - k_7} = \frac{(A - A_{set})}{k_6 + A} = -\frac{(A_{set} - A)}{k_6 + A} \tag{1.9}$$

$$\dot{E} = -\underbrace{\frac{(k_5 - k_7)}{K_6 + A}}_{\gamma_A} \cdot \underbrace{(A_{set} - A)}_{error} \tag{1.10}$$

$$if \quad \dot{E} \rightarrow 0 \ , \quad A \rightarrow A_{set} \tag{1.11}$$

$$\frac{dE}{dt} = \gamma \left(A_{set} - A\right) \tag{1.12}$$

$$\frac{\dot{E}}{k_6 k_7} = \frac{\frac{(k_5 - k_7) \cdot A}{k_6 K_7} - 1}{k_6 + A} \tag{1.13}$$

To compensate the perturbing flux j_9=k_9; a larger compensating flux j_2 flux $(k_2\mathrm{P}/(k_3+\mathrm{P}))\cdot(\mathrm{k}_4/(k_4+\mathrm{E}))$ is needed to compensate; otherwise the concentration of A would not reach $\mathrm{A_{set}}$.

The figure below shows how the system is trying to maintain the controlled variable A in its setpoint with help of motif 2 controlling system, where controlling variable E decreases to reduce ("derepress") the inhibition of the compensatory flux j_2. This reduction in variable E continues by raise of outflow perturbation until variable E becomes zero, so it cannot decrease any more and the controller breaks down [24].

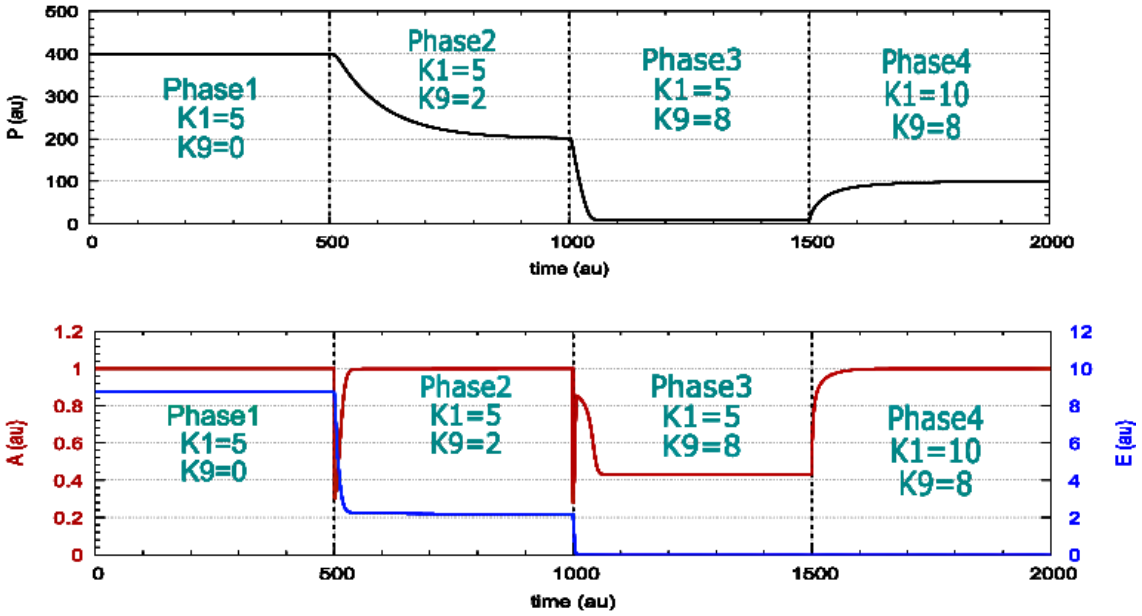

FIGURE 1.7: Robust Homeostasis of A during stepwise increases of perturbation k_9. The concentration of manipulated variable E decreases by derepression in order to diminish the inhibition on the compensatory flux j_2 to keep A at its setpoint. When the controller variable E goes to zero, the controller system breaks down. It means that in phase 3, the controller variable is no longer available to compensate for the increasing outflow perturbation. In this study, by raising k_1 and inflow of P in phase 4, A goes toward its homeostasis. k_1 and k_9 values are shown on the plot. Other rate constants are: k_2=10, k_3=10, k_4=1, k_5= 2, k_6=1, k_7=1, k_8= 1×10^{-6}, k_{10}=1×10^{-2}, A_{set}=1.0

1.4.1 Hysteretic behaviour of dopamine release into the synaptic cleft

Hysteretic behaviour was first suggested by Neet et al for enzyme response to changes. Enzyme activity does not show a linear increase or decrease by substance changes [25]. Initial velocity on substrate concentration reaction rate to the binding sites of enzymes showed to have a sigmoidal dependence. This slow transition may limit the overall reaction rate [26]. Justice et al. studied the dopamine release into the synaptic cleft in the rat brain. They measured the relationship between 10 second stimulus of the neurons in the medial forebrain and the concentration of extracellular dopamine [27]. Best et al. did another research, and compared their results with the results from Justice et al. experiment [7]. Both researches shows sigmoidal and hysteretic properties in dopamine release. Dopamine levels start to increase slightly after starting the electrical stimulus and decrease slightly. Best et al. found that dopamine starts to decrease before the end of electrical stimulation due to depletion of vesicular dopamine reservoir [7]. This feature of dopamine release will be further discussed in the Results and Discussion.

In this study, TH-DA negative feedback regulation and robust homeostasis of DOAP is illustrated. Also by modelling these molecules behaviour and different calculations, DA regulation in the presynaptic neuron, and dopamine release into the synaptic cleft has been studied.

Chapter 2

Materials and Methods

2.1 Method of calculation

Rate equations were solved by using the Fortran subroutine (LSODE). Plots and curves were generated with gnuplot (www.gnuplot.info) and annotated with Inkscape (www.inkscape.org). Concentrations are denoted by the compound names without brackets and are given in μM and time units are in minutes.

2.2 Model of DOPA regulation

As it has been mentioned earlier, in the introduction, that dopamine is stored and released in wide and complex structures of dopaminergic neurones in the midbrain [6]. The main focus of this study, is to investigate the dopamine synthesis and regulation in the axonal structure and to demonstrate how dopamine release behaves in the synaptic cleft. This study assumes that enzymes TH, DDC and VMAT-2 are parts of a channeling complex as shown in Figure 1.3. To implement the robust homeostasis, we need dopamine removal (TH-inhibititor) by zero-order kinetics, which is dopamine loading to the vesicle by enzyme VMAT-2. In this study, dopamine is the controller and DOPA is the controlled species which is demonstrated in Figure 1.6.

Figure 2.1 shows an overview of considered TH-DA regulation.

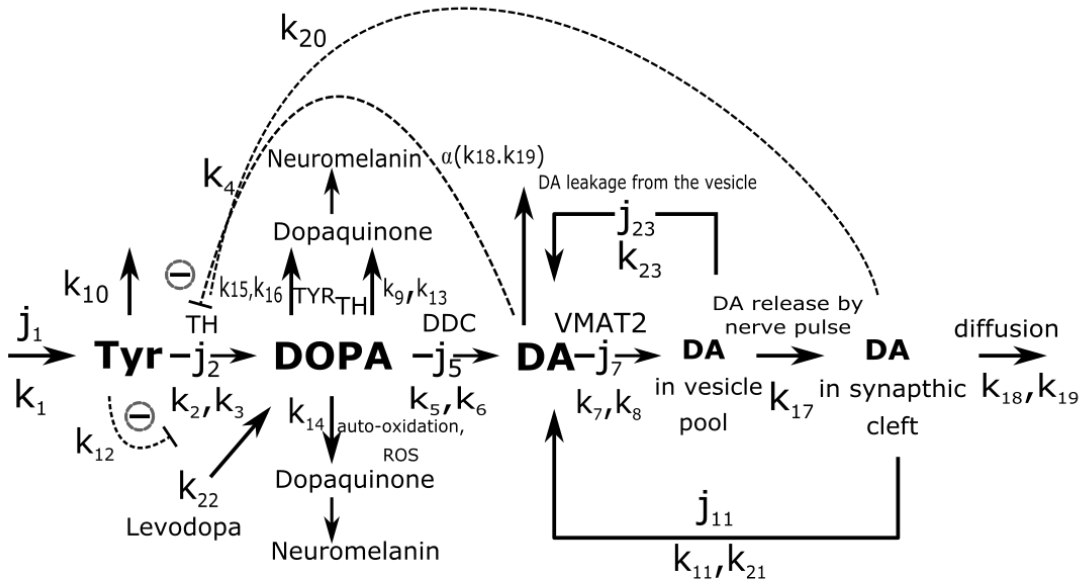

FIGURE 2.1: This model shows a reaction scheme, from amino-acid tyrosine to DOPA, converting DOPA to DA by DDC. DA then moves to the synapthic vesicle pools, releasing in the synapthic cleft by receiving an inflow of calcium ions by neuronal stimulation. Finally, removal of dopamine from the synapthic cleft by autoreceptors and DAT. In this model, pairs of rate constant (k_i, k_j) represents respectively (V_{max}, K_M)values of Michaelis-Menten kinetics.

To implement robust homeostasis in this TH-DA negative feedback loop, zero-oreder kinetics of removal of dopamine is needed. Experimentally determined value of k_M for the enzyme VMAT2 (k_8) shows the value of (0.29 μM) which is consistent with this concept [28].

2.3 Parameter values

K_M values have been found in literature, from experimentally determinations. V_{max} values are concentration based and mostly unknown. Rate constants k_1, k_{10}, k_{11}, k_{14}, k_{17}, k_{20}, k_{22} are adjustable parameters.

2.3.1 TH K_M value: k_3

In the enzyme database BRENDA, There are 16 k_M values for TH for homo sapiens using L-Tyrosine as substrate. values vary from 0.0081 mM to 0.166 mM. In this study,

an average value of 0.0744 mM (74.4 μM) has been used [29].

2.3.2 Inhibition of TH by DA: k_4

The inhibition constant for dopamine is dependent on the enzyme's phosphorylation status[30]. TH is maintained in homeostasis in posttranslational status, by feedback inhibition by catecholamines and phosphorylation at Serine/Threonine residues in N-terminal [31]. In the S40 phosphorylated form, inhibition constant for dopamine is between 78-208 μM. In the unphosphorylated enzyme, dopamine binding is more irreversible, the inihibiton constant is much lower, for example lower than 0.0035μM [32].

2.3.3 Dopadecarboxylase(DDC) K_M value:k_6 and Vmax: k_5

BRENDA shows k_M values for DDC for substrate LDOPA between 0.028 μM and 4.27 μM. Multiplicative average of these values is used in the calculation, k_6=$\sqrt{0.028 \times 4.27}\mu$M= 0.306 μM. The turnover number of the enzyme is determined 5.1 s^{-1} [33]. If we assume DDC concentration of 10^{-8}M, V_{max} is 3.06 μM/min. k_5 is assumed to be 10μM in the calculation.

2.3.4 Dopamine loading to the vesicle by VMAT-2 and leakage from vesicle

Robust homeostasis of DOPA can be seen when VMAT-2 K_M value is very low compare to the dopamine concentration. The K_M was determined by voltammetry for dopamine uptake to the vesicle is 0.289 μM and V_{max} is 1.9fmol/(s.mg protein). [28]. Cytosolic dopamine concentration determined to be between 2 and 3μM [34] and 47-140μM [35]. It has been shown that dopamine and other neurotransmitters strored in the vesicle may leak out from the vesicle into the cytoplasm (k_{23}) [36]. We use the K_M value of (0.0158$\pm$0.0006) min^{-1} based on Schon et. al studies [36].

2.3.5 Inhibition of TH by Tyr: k_{12}

BRENDA lists five inhibition constants for TH by Tyrosine. values are 37 μM, 44 μM, 46 μM, 48 μM, 73 μM. The average value of 50 μM is used in my calculations.

2.3.6 Tyrosinase (TYR) K_M and V_{max} values: k_9, k_{13}

There are 3 K_M entries reported for TYR with DOPA as a substrate. 340 μM [37], 480 μM and 490 μM [38]. Average value of 437 μM is used in this model calculation. Turnover number is reported to be 38.11 S^{-1} [37]. The concentration using in the calculation is 10^{-9} μM and V_{max} value is 2.3 μM/min.

2.3.7 DOPA oxidation by TH K_M and V_{max}

DOPA oxidation by TH is reoprted to be 56±12 μM [39]. V_{max} for TH converting DOPA is used the same value as TYR removal of DOPA: 2.3 μM/min.

2.3.8 Dopamine re-entry by DAT, k_{11} and k_{21}

DAT (dopamine transporter) has shown to follow Michaelis-Menten kinetics with K_M value between 0.2 to 2 μM [40]. We assumed k_{21} close to zero in this calculation to to model dopamine returning to the presynaptic cell by zero-order conditions. However, different values of k_{21} can alter $DOPA_{set}$.

2.3.9 MAO removing dopamine: k_{19}

As it is mentioned earlier, the cytosolic concentration of dopamine is low(2-3 μM)and the k_m of removal of DA is high,(determined K_M value for the MAO is 111μM), I assumed that the removal should be linear with V_{max}: 90 μM/min for 1 μM concentration of MAO[41].

2.3.10 Dopamine release by receiving nerve pulse k_{17}

In the calculations regarding hysteretic decrease of dopamine, experimentally determined values for k_{17} have been used and it is not adjustable variable anymore. K_{17}^{low} is close to zero and value of 10^{-6} have been used. K_{17}^{high} has the value of 5.64×10^{-4}. L_{17} is assumed to be 30.

2.4 The rate equations

The rate equations for the model in Figure 2.1 are:

$$\frac{d(Tyr)}{dt}=k_1-\left(\frac{k_2\cdot Tyr}{k_3\left(1+\frac{DA}{k_4}\right)\cdot\left(1+\frac{DOPA}{k_{16}}\right)+Tyr}\right)\left(\frac{k_{12}}{k_{12}+Tyr}\right)\left(\frac{k_{20}}{k_{20}+DA_{ex}}\right)-k_{10}\cdot Tyr \tag{2.1}$$

$$\frac{d(DOPA)}{dt}=\left(\frac{k_2\cdot Tyr}{k_3\left(1+\frac{DA}{k_4}\right)\cdot\left(1+\frac{DOPA}{k_{16}}\right)+Tyr}\right)\left(\frac{k_{12}}{k_{12}+Tyr}\right)\left(\frac{k_{20}}{k_{20}+DA_{ex}}\right) -\frac{k_9\cdot DOPA}{k_{13}+DOPA}-\frac{k_5\cdot DOPA}{k_6+DOPA}-k_{14}\cdot DOPA-\frac{k_{15}\cdot DOPA}{k_{16}\left(1+\frac{Tyr}{k_3}\right)+DOPA}+k_{22} \tag{2.2}$$

$$\frac{d(DA)}{dt}=\frac{k_{11}\cdot DA_{ex}}{k_{21}+DA_{ex}}+\frac{k_5\cdot DOPA}{k_6+DOPA}-\frac{k_7\cdot DA}{k_8+DA}-\alpha\cdot\frac{k_{18}\cdot DA}{k_{19}+DA}+k_{23}\cdot(DA_{ves}) \tag{2.3}$$

$$\frac{d(DA_{ves})}{dt}=\frac{k_7\cdot DA}{k_8+DA}-k_{17}\cdot DA_{ves}-k_{23}\cdot(DA_{ves}) \tag{2.4}$$

$$\frac{d(DA_{ex})}{dt}=k_{17}\cdot DA_{ves}-\frac{k_{18}\cdot DA_{ex}}{k_{19}+DA_{ex}} \tag{2.5}$$

By solving Equation for DOPA, if d(DA) / dt = 0, equation 2.6 will be the DOPA set-point. This equation shows factors directly effective on DOPA_{set}.

$$DOPA_{set}=\frac{k_6(k_7-j_{11}-j_{23})}{k_5+j_{11}+k_{23}-k_7} \tag{2.6}$$

The following equation used to show hysteretic (a time dependent) behaviour in dopamine release from the presynaptic neuron.

$$\mathrm{k_{17}}=\mathrm{k_{17}}^{\mathrm{high}}(1-\mathrm{e}^{\mathrm{k_{17}\cdot t}})+\mathrm{k_{17}}^{\mathrm{low}} \tag{2.7}$$

Chapter 3

RESULTS

3.1 Various factors influencing DOPA homeostasis

3.1.1 Illustrating the influence of VMAT2 K_M on DOPA homeostasis

k_8 value, the K_M of enzyme VMAT2, catalysing dopamine loading to the vesicle, is one of the necessary factors in robust homeostasis of DOPA. Dopamine transport to the vesicle should be zero-order with respect to dopamine. In Figures 3.1 to 3.3, the influence of K_M, in maintaining the DOPA in its set point has been shown. This study, has 3 phases and DOPA perturbation(ROS) is raising from phase 1 to the phase 3. In the first model, k_8 is the actual experimentally [28] determined value. Perturbation (ROS, k_{14}) is raising from phase 1 to phase 3 as 0.0 min^{-1}, 0.01 min^{-1}, 0.1 min^{-1} respectively. The controller keeps DOPA at its set-point from phase 1 to phase 3.

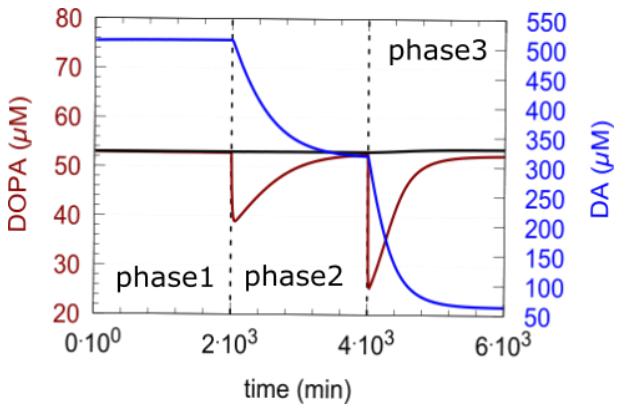

FIGURE 3.1: Controler's accuracy dependence on k_8 value. Black line shows DOPA set-point. Despite successive raise of perturbation (ROS, k_{14}) in 3 phases, DOPA stays in its set point and controller compensate for outgoing amount of dopamine. Rate constants are as following: k_1=10 μM/min, k_2=1000.0 μM/min, k_3=74.4 μM, k_4=6 μM (phosphorylated form of TH), k_5=3.1 μM/min, k_6=346 μM, k_7=1.5 μM/min,k_8=0.29μM, k_9=2.3 μM/min, k_{10}=0.025 min^{-1}, k_{11}=1 μM/min, k_{12}=50 μM, k_{13}=437 μM, k_{14} phase 1: 0.0 min^{-1}, k_{14} phase 2: 0.01 min^{-1}, k_{14} phase 3: 0.1 min^{-1}, k_{15}=2.3 μM/min, k_{16}=56 μM, k_{17}=0.01 min^{-1}, k_{18}=90 μM/min, k_{19}=111 μM, k_{20}=0.1 μM, k_{21}=1$\times$10^{-4}μM, k_{22}=0.0 min^{-1}. These rate constant values give a $DOPA_{set}$ (Equation 2.6) of 53.3μM. Initial concentrations: Tyr=352.0 μM, $DOPA$=66.5 μM, DA=167.9 μM, DA_{ves}=150 μM, DA_{ex}=0.62 μM.

The results of this experimentally determined study, shows that in presence of different perturbation, controller has the ability to compensate and help DOPA goes back to its set-point. This controller system is possible by very low amounts of k_8. Transporting DA into the vesicle by VMAT with zero-order kinetics is one necessary condition for the controller performance.

In the Figure 3.2, k_8 is decreased by one order of magnitude (A) and two orders of magnitude (B). In both models, k_8 is getting closer to zero which is in favour of VMAT2 zero-order conditions. The controller continues working accurately from phase 1 to phase 3. The k_8 value for plot A and B is 2.9$\times$10^{-3}μM and k_8=2.9$\times$10^{-3}μM respectively. Other rate constants and initial concentrations are exactly the same as Figure 3.1.

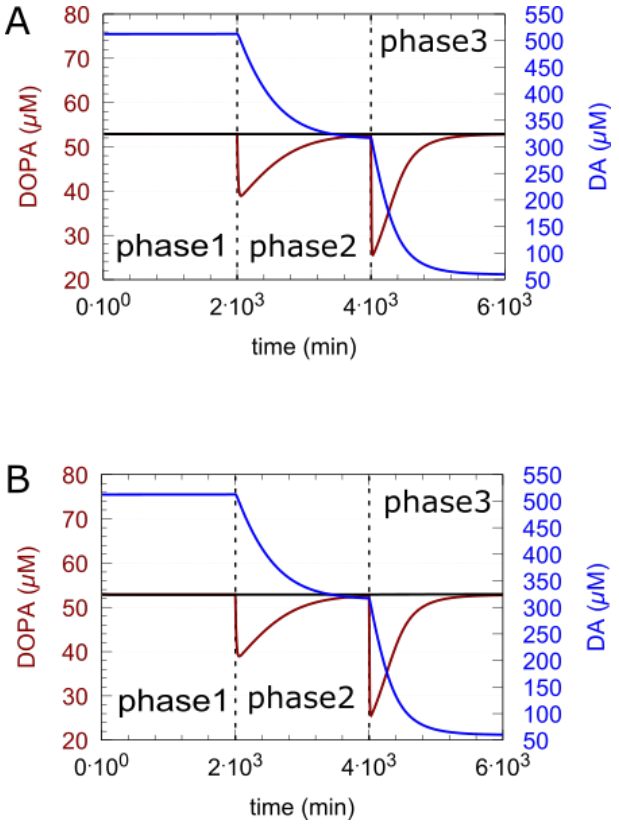

FIGURE 3.2: controler's accuracy dependence on K8 value. Black line shows DOPA set point. Despite successive raise of perturbation(ROS, k_{14} in 3 phases, DOPA stays in its set point and controller compensate for outgoing amount of dopamine.k_8(A)=0.029, (B)=0.0029. Other rate constants are as following: k_1=10 μM/min, k_2=1000.0 μM/min, k_3=74.4 μM, k_4=6 μM (phosphorylated form of TH), k_5=3.1 μM/min, k_6=346 μM, k_7=1.5 μM/min, k_9=2.3 μM/min, k_{10}=0.025min^{-1}, k_{11}=1 μM/min, k_{12}=50 μM, k_{13}=437 μM, k_{14} phase 1: 0.0 min^{-1}, k_{14} phase 2: 0.01 min^{-1}, k_{14} phase 3: 0.1 min^{-1}, k_{15}=2.3 μM/min, k_{16}=56 μM, k_{17}=0.01min^{-1}, k_{18}=90 μM/min, k_{19}=111 μM, k_{20}=0.1 μM, k_{21}=1$\times$10^{-4}μM, k_{22}=0.0 min^{-1}. These rate constant values give a $DOPA_{set}$ (Equation 2.6) of 66.6μM. Initial concentrations for both plots are: Tyr=352.0 μM, $DOPA$=66.5 μM, DA=167.9 μM, DA_{ves}=150 μM, DA_{ex}=0.62 μM.

In the third experiment, the value of k_8 is raised by 1 order of magnitude instead of being lowered as it was in the second experiment. High values of k_8 are not in favour of zero-order kinetics of dopamine loading into the vesicle by enzyme VMAT2. As has been shown in Figure 3.3, By raising the perturbation (ROS, k_{14}), in phase 3, the controller system becomes less accurate and DOPA steady state goes far from its set-point.

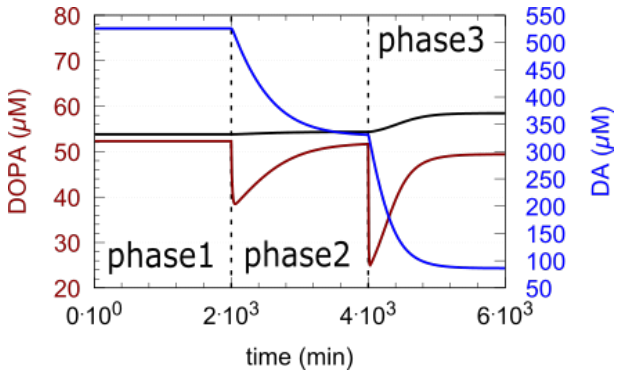

FIGURE 3.3: Lower controller accuracy by raising k_8 value by 1 order of magnitude. Black line shows DOPA set point. With successive raise of perturbation (ROS, k_{14} in 3 phases, controller tends to break down due to high value of k_8. Rate constants are as following: k_1=10 μM/min, k_2=1000.0 μM/min, k_3=74.4 μM, k_4=6 μM (phosphorylated form of TH), k_5=3.1 μM/min, k_6=346 μM, k_7=1.5 μM/min,k_8=2.9μM, k_9=2.3 μM/min, k_{10}=0.025min^{-1}, k_{11}=1 μM/min, k_{12}=50 μM, k_{13}=437 μM, k_{14} phase 1: 0.0 min^{-1}, k_{14} phase 2: 0.01 min^{-1}, k_{14} phase 3: 0.1 min^{-1}, k_{15}=2.3 μM/min, k_{16}=56 μM, k_{17}=0.01min^{-1}, k_{18}=90 μM/min, k_{19}=111 μM, k_{20}=0.1 μM, k_{21}=1×10^{-4}μM, k_{22}=0.0 min^{-1}. These rate constant values give a $DOPA_{set}$ (Equation 2.6) of 54μM. Initial concentrations: Tyr=324.0 μM, $DOPA$=52.3 μM, DA=526 μM, DA_{ves}=231 μM, DA_{ex}=1.64 μM.

Figures 3.1 to 3.3 shows that the goal of this controlling system seems to be maintaining DOPA steady states near its set-point, while DA values, as controller variable are changing in presence of perturbation.

3.1.2 Illustrating the influence of compensatory flux j_2 on DOPA homeostasis.

As it has been discussed earlier and shown by the equation **??**, the compensatory flux j_2 has a very important role in derepression and compensating the outgoing amounts of DOPA in the controller. The higher j_2 is, the more controller is able to compensate the loss of dopamine in the controlling system.

$$j_2 = \left(\frac{k_2 \cdot Tyr}{k_3 \left(1+\frac{DA}{k_4}\right) \cdot \left(1+\frac{DOPA}{k_{16}}\right) + Tyr} \right) \left(\frac{k_{12}}{k_{12}+Tyr} \right) \left(\frac{k_{20}}{k_{20}+DA_{ex}} \right) \tag{3.1}$$

As it has been shown in the equation 3.1, one of the most important factors effective in performing compensatory fluxj_2 is the incoming concentration of Tyrosine to the controller system. Increasing concentration of Tyrosine has negative effect on compensatory flux j_2 and it causes to decrease the flux j_2. To show how this increase can affects on the controller, in the next experiment, k_1 is increased by one order of magnitude in

comparison with the reference experiment shown in Figure 3.1. all other rate constants are the same as Figure 3.1.

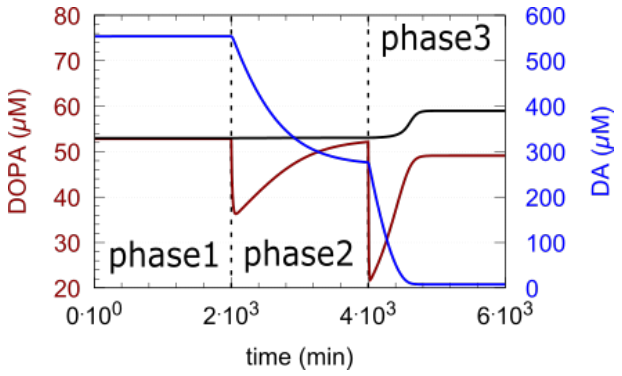

FIGURE 3.4: Lower controller accuracy by increasing k_1 value by 1 order of magnitude. Black line shows DOPA set point. With successive raise of perturbation (ROS, k_{14} in 3 phases, controller tends to break down due to high levels of Tyrosine inflow. Rate constants are as following: k_1=100 μM/min, k_2=1000.0 μM/min, k_3=74.4 μM, k_4=6 μM (phosphorylated form of TH), k_5=3.1 μM/min, k_6=346 μM, k_7=1.5 μM/min,k_8=0.29μM, k_9=2.3 μM/min, k_{10}=0.025min^{-1}, k_{11}=1 μM/min, k_{12}=50 μM, k_{13}=437 μM, k_{14} phase 1: 0.0 min^{-1}, k_{14} phase 2: 0.01 min^{-1}, k_{14} phase 3: 0.1 min^{-1}, k_{15}=2.3 μM/min, k_{16}=56 μM, k_{17}=0.01min^{-1}, k_{18}=90 μM/min, k_{19}=111 μM, k_{20}=0.1 μM, k_{21}=1$\times$10^{-4}μM, k_{22}=0.0 min^{-1}. These rate constant values give a $DOPA_{set}$ (Equation 2.6) of 53μM at the end of phase 1 and 2, and 59 μM at the end of the third phase. Initial concentrations: Tyr=3936.0 μM, $DOPA$=52.8 μM, DA=554 μM, DA_{ves}=232 μM, DA_{ex}=1.65μM.

This properties of the controller system help DOPA maintain its set-point after eating meals with high concentrations of aminoacid tyrosine [7].

3.1.3 Illustrating the Tyrosine Hydroxylase inhibition by dopamine

As is mentioned earlier in "Materials and Methods", k_4 inhibition in this model is dependent on TH phosphorylation status. The inhibition (dissociation) constant for the non-phosphorylated enzyme is lower (much stronger dopamine inhibition). In this experiment, all the k values are exactly the same as the first experiment shown in Figure 3.1, but the k_4 value is decreased by one order of magnitude. Figure 3.5 shows that TH inhibition results in less compensatory flux and less DOPA set-point, in comparison with experiment number one. Figure 3.5 shows the behaviour of the system in low K_M values and figure 3.6 clarifies the differences between these two experiments.

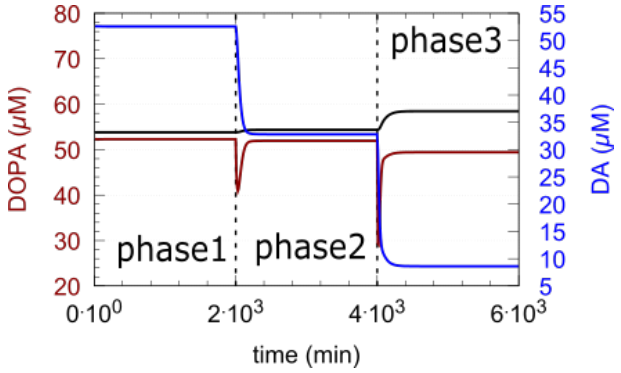

FIGURE 3.5: This figure shows how decrease of k_4 leads to poorer homeostasis of DOPA. All rate constants are the same as experiment 1, exceptc k_4=0.6 μM/min,k_1=10μM/min, k_2=1000.0 μM/min, k_3=74.4 μM, k_5=3.1 μM/min, k_6=346 μM, k_7=1.5 μM/min,k_8=2.9μM, k_9=2.3 μM/min, k_{10}=0.025min^{-1}, k_{11}=1 μM/min, k_{12}=50 μM, k_{13}=437 μM, k_{14} phase 1: 0.0 min^{-1}, k_{14} phase 2: 0.01 min^{-1}, k_{14} phase 3: 0.1 min^{-1}, k_{15}=2.3 μM/min, k_{16}=56 μM, k_{17}=0.01min^{-1}, k_{18}=90 μM/min, k_{19}=111 μM, k_{20}=0.1 μM, k_{21}=1$\times$10^{-4}μM, k_{22}=0.0 min^{-1}. These rate constant values give a $DOPA_{set}$ (Equation 2.6) of 53.8 μM at the end of the phase 1, 54.3 μM at the end of phase 2 and 58.5 μM at the third phase. Initial concentrations: Tyr=3240.0 μM, $DOPA$=523 μM, DA=52.6 μM, DA_{ves}=231 μM, DA_{ex}=1.6 μM.

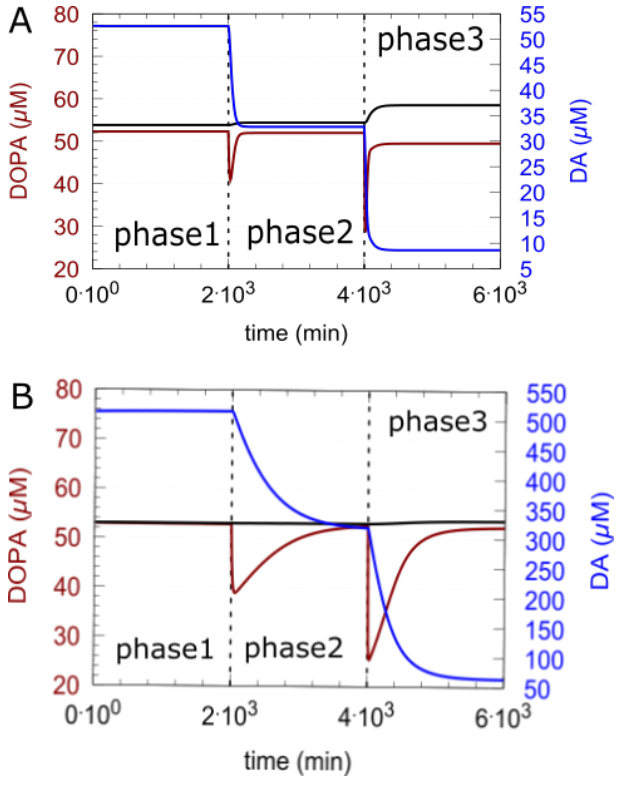

FIGURE 3.6: (A): Decrease of k_4 by one order of magnitude (0.6μM/min) in comparison with (B): k_4=6μM/min. All other rate constants are the same as experiment number1 3.1. Plot (B) has the $DOPA_{set}$ and initial concentrations exactly the same as first experiment. $DOPA_{set}$ for plot (A) is 53.8μM at the end of the phase 1, 54.3 μM at the end of phase 2 and 58.5μM at the third phase. Initial concentrations for plot (A): Tyr=3240.0 μM, $DOPA$=523 μM, DA=52.6 μM, DA_{ves}=231 μM, DA_{ex}=1.6 μM.

Figure 3.6 shows the effect of decreasing k_4, for example, by de-phosphorylation of enzyme TH. This decrease cause higher inhibition of TH, in consequence, lower dopamine steady-state levels. Also faster response of the DOPA to the controller can be seen in the plot (A).

To illustrate how higher values of k_4 can affect the controller, for example, by phosphorylation, next experiment has done with increase of k_4 to (45 μM/min) in comparison with the reference experiment shown in Figure 3.1.

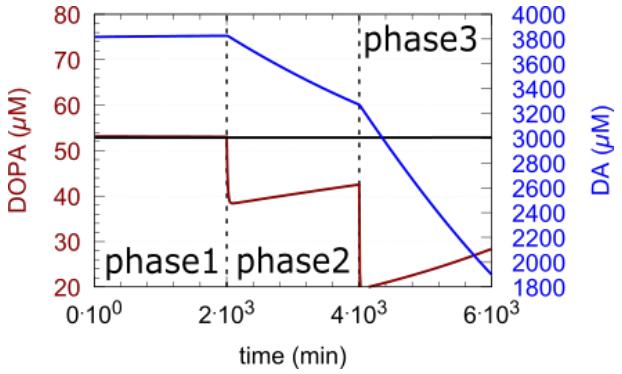

FIGURE 3.7: Controller response to compensate perturbation in 3 phases(ROS, k_{14}) is much slower with higher k_4 values . Black line shows DOPA set point. k_4 is 45μM. k_1=10 μM/min, k_2=1000.0 μM/min, k_3=74.4 μM, μM, k_5=10 μM/min, k_6=346 μM, k_7=6 μM/min,k_8=0.29μM, k_9=2.3 μM/min, k_{10}=0.025min^{-1}, k_{11}=1 μM/min, k_{12}=50 μM, k_{13}=437 μM, k_{14} phase 1: 0.0 min^{-1}, k_{14} phase 2: 0.02 min^{-1}, k_{14} phase 3: 0.12 min^{-1}, k_{15}=2.3 μM/min, k_{16}=56 μM, k_{17}=0.01min^{-1}, k_{18}=90 μM/min, k_{19}=111 μM, k_{20}=0.1 μM, k_{21}=1$\times$10^{-4}μM, k_{22}=0.0 min^{-1}, k_{23}=0.0158μM. These rate constant values give a $DOPA_{set}$ (Equation 2.6) of 52.8μM in the last phase. Initial concentrations: Tyr=323.0 μM, $DOPA$=53.1 μM, DA=3187 μM, DA_{ves}=232.5 μM, DA_{ex}=1.65 μM

Figure 3.7, shows very slow response in compensating perturbation. Figure 3.8 illustrates how the controller works in higher values of k_4 with longer time in each phase. This experiment is performed only in two phases. Phase 2 is long enough to let DOPA goes back close to its set-point.

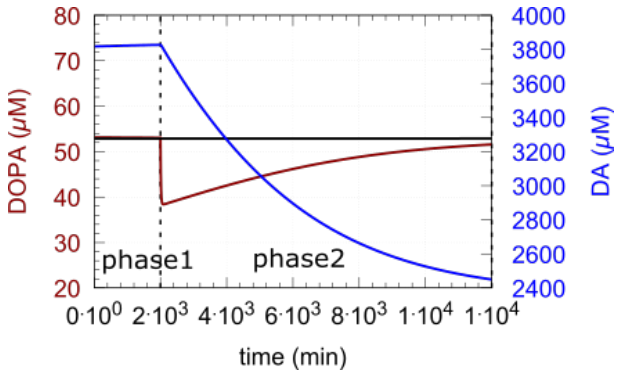

FIGURE 3.8: Extending phase 2 to illustrate the controller behaviour in 2 phases. Black line shows DOPA set point. k_4 is 45μM. k_1=10 μM/min, k_2=1000.0 μM/min, k_3=74.4 μM, k_5=10 μM/min, k_6=346 μM, k_7=6 μM/min,k_8=0.29 μM, k_9=2.3 μM/min, k_{10}=0.025 min^{-1}, k_{11}=1 μM/min, k_{12}=50 μM, k_{13}=437 μM, k_{14} phase 1: 0.0 min^{-1}, k_{14} phase 2: 0.02 min^{-1}, k_{15}=2.3 μM/min, k_{16}=56 μM, k_{17}=0.01 min^{-1}, k_{18}=90 μM/min, k_{19}=111 μM, k_{20}=0.1 μM, k_{21}=1$\times$10^{-4}μM, k_{22}=0.0 min^{-1}, k_{23}=0.0158 μM. These rate constant values give a $DOPA_{set}$ (Equation 2.6) of 52.8μM in the last phase. Initial concentrations: Tyr=323.0 μM, $DOPA$=53.1 μM, DA=3187 μM, DA_{ves}=232.5 μM, DA_{ex}=1.65 μM

3.1.4 Adding dopamine to the system by Levodopa treatment

One way to treat any kind of decrease in DOPA, for example, when for any reason there is a decrease in TH activity, like TH deficiency (THD) [42], or, in a disease like DOPA-responsive dystonia (DRD)[43], is to use the external DOPA, as a medication like Levodopa which has been shown as k_{22} in this model. In this experiment, different effects of LDOPA treatment has been shown. This experiment illustrates two different behaviours. If j_5+j_{11}+j_{23} is lower than loading the DA to the vesicle j_7, LDOPA helps the DOPA remain in values more close to $DOPA_{set}$. Figures 3.9 and 3.10 shows the difference between controller behaviour with and without adding LDOPA. In both figures, plot (A) shows the controller system without LDOPA addition and plot (B) shows where LDOPA is added to the system. Also influence of the controller accuracy (k_8 value) can be compared between Figure 3.9 and 3.10. k_8 value has an important role in how LDOPA effect the system regulation. In Figure 3.10 , the accuracy is high (lower k_8 value), so LDOPA has better performance, DOPA is more close to its set-point and dopamine has higher levels.

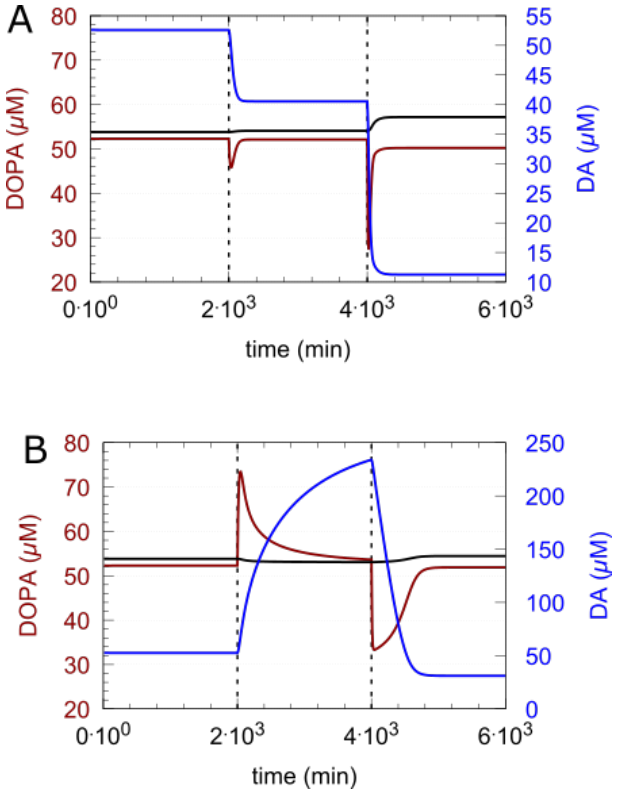

FIGURE 3.9: (A) controller without LDOPA treatment with k_{22}=0 from phase 1 to phase3. (B) shows the controller performance by adding LDOPA treatment. k_{22} phase1=0 min^{-1}, phase2=2 min^{-1}, phase3=4 min^{-1} .k_8 value the same as experiment 1: 0.29 μM. Other rate constants are as following: k_1=10 μM/min, k_2=10000 μM/min, k_3=74.4 μM, k_4=0.6 μM (phosphorylated form of TH), k_5=10 μM/min, k_6=346 μM, k_7=6 μM/min, k_9=2.3 μM/min, k_{10}=0.025 min^{-1}, k_{11}=1 μM/min, k_{12}=50 μM, k_{13}=437 μM, k_{14} phase 1: 0.0 min^{-1}, k_{14} phase 2: 0.01 min^{-1}, k_{14} phase 3: 0.1 min^{-1}, k_{15}=2.3 μM/min, k_{16}=56 μM, k_{17}=0.01min^{-1}, k_{18}=90 μM/min, k_{19}=111 μM, k_{20}=0.1 μM, k_{21}=1×$10^{-4}$$\mu$M, k_{23}=0.0158 μM. These rate constant values give a $DOPA_{set}$ (Equation 2.6) for(A)=57.16μM, (B)=54.4μM. Initial concentrations: Tyr=324.0 μM, $DOPA$=52.3 μM, DA=52.6 μM, DA_{ves}=231 μM, DA_{ex}=1.6 μM.

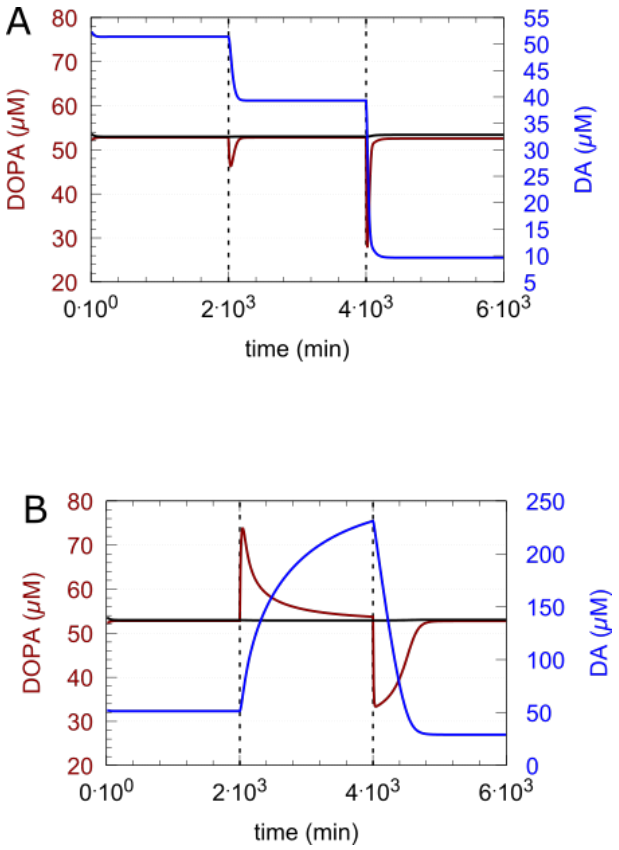

FIGURE 3.10: (A)controller without LDOPA treatment with k_{22}=0 from phase 1 to phase3. (B) shows the controller performance by adding LDOPA treatment phase1=0min^{-1}, phase2=2min^{-1}, phase3=4min^{-1} .k_8 value is lower than previous figure in both plots: 0.029μM, so the controller has better accuracy. Other rate constants are as following: k_1=10 μM/min, k_2=10000 μM/min, k_3=74.4 μM, k_4=0.6 μM (phosphorylated form of TH), k_5=10 μM/min, k_6=346 μM, k_7=6μM/min, k_9=2.3 μM/min, k_{10}=0.025min^{-1}, k_{11}=1 μM/min, k_{12}=50 μM, k_{13}=437 μM, k_{14} phase 1: 0.0 min^{-1}, k_{14} phase 2: 0.01 min^{-1}, k_{14} phase 3: 0.1 min^{-1}, k_{15}=2.3 μM/min, k_{16}=56 μM, k_{17}=0.01min^{-1}, k_{18}=90 μM/min, k_{19}=111 μM, k_{20}=0.1 μM, k_{21}=1$\times$10^{-4}μM. These rate constant values give a $DOPA_{set}$ (Equation 2.6) of(A)= 53.4 μM(B)=53.0 μM. Initial concentrations: Tyr=324.0 μM, $DOPA$=52.3 μM, DA=52.6 μM, DA_{ves}=231 μM, DA_{ex}=1.6 μM.

When external dopa addition like Levodopa is in higher values than loading the dopa to the vesicle, the controller breaks down. DA levels grow continuously and DOPA steady state is higher than $DOPA_{set}$. In this situation, the controller system tries to decrease the DA levels by decreasing the compensatory flux, which is applicable by increasing DA but leads to high, uncontrolled amount of DA.

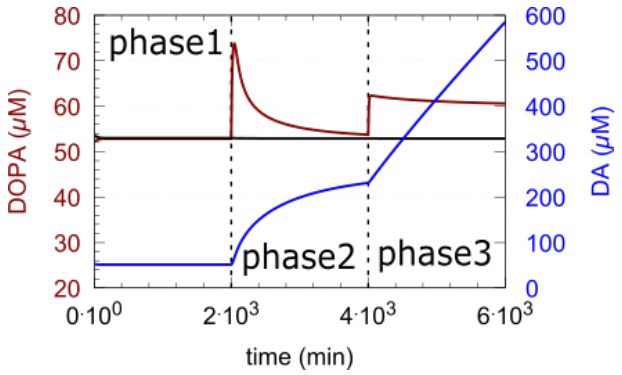

FIGURE 3.11: Breaking the controller by adding too much Ldopa to the system, even with high controller accuracy, k_8=0.029. Black line shows DOPA set point. Other rate constants are as following: k_1=10 μM/min, k_2=10000 μM/min, k_3=74.4 μM, k_4=0.6 μM (phosphorylated form of TH), k_5=10 μM/min, k_6=346 μM, k_7=6μM/min, k_9=2.3 μM/min, k_{10}=0.025min^{-1}, k_{11}=1 μM/min, k_{12}=50 μM, k_{13}=437 μM, k_{14} phase 1: 0.0 min^{-1}, k_{14} phase 2: 0.01 min^{-1}, k_{14} phase 3: 0.1 min^{-1}, k_{15}=2.3 μM/min, k_{16}=56 μM, k_{17}=0.01 min^{-1}, k_{18}=90 μM/min, k_{19}=111 μM, k_{20}=0.1 μM, k_{21}=1$\times$10^{-4}μM, k_{22}=phase1: 0.0 min^{-1}, phase2: 2.0 min^{-1}, phase3:8.0 min^{-1}. These rate constant values give a $DOPA_{set}$ (Equation 2.6) of 52.88 μM. Initial concentrations: Tyr=324.0 μM, $DOPA$=52.3 μM, DA=52.6 μM, DA_{ves}=231 μM, DA_{ex}=1.6 μM

3.1.5 Influence of DA removal/ Auto-oxidation on DOPA homeostasis

Auto-oxidation and DA removal by oxidative enzymes like MAO, leads to deteriorated DOPA homeostasis. However, channeling complex of enzymes may protect DOPA and DA from ROS and MAO. In the Figure 2.1, removal of DA by MAO and auto-oxidation has been shown. Figure 3.12, shows that in presence of MAO and Aauto-oxidation, DA goes to zero and system is unable to decrease DA to compensate the lower concentrations of DOPA. In this conditions, controller breaks down.

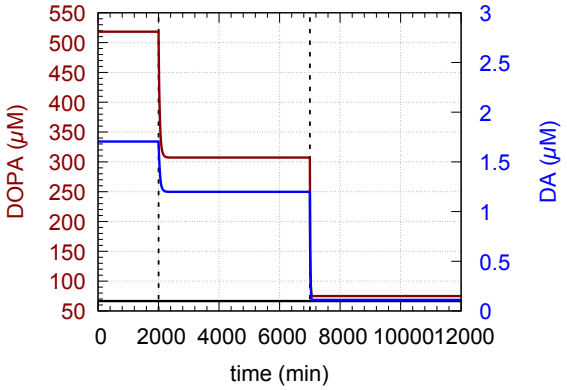

FIGURE 3.12: Influence of MAO and Auto-oxidation on the controller stability. Rate constants are as following: k_1=10 μM/min, k_2=1000.0 μM/min, k_3=74.4 μM, k_4=6 μM (phosphorylated form of TH), k_5=3.1 μM/min, k_6=346 μM, k_7=1.5 μM/min,k_8=0.29μM, k_9=2.3 μM/min, k_{10}=0.025 min^{-1}, k_{11}=1 μM/min, k_{12}=50 μM, k_{13}=437 μM, k_{14} phase 1: 0.0 min^{-1}, k_{14} phase 2: 0.01 min^{-1}, k_{14} phase 3: 0.1 min^{-1}, k_{15}=2.3 μM/min, k_{16}=56 μM, k_{17}=0.01 min^{-1}, k_{18}=90 μM/min, k_{19}=111 μM, k_{20}=0.1 μM, k_{21}=1$\times$10^{-4}μM, k_{22}=0.0 min^{-1}. These rate constant values give a $DOPA_{set}$ (Equation 2.6) of 53.3μM. Initial concentrations: Tyr=211.0 μM, $DOPA$=520 μM, DA=1.82 μM, DA_{ves}=150 μM, DA_{ex}=0.62 μM.

3.2 Dopamine release to the synaptic cleft

In the Figure 2.1 k_{17} has been shown as the rate constant of the flux for dopamine release into the synaptic cleft. As it has been discussed earlier in the introduction, there is an inflow of Ca^{2+} ions to the cell by receiving an action potential and through voltage-gated channels. By raising the concentration of the Ca^{2+} in the nerve terminal, dopamine vesicle fuse to the cell membrane and release dopamine by the exocytosis. However, performing all these steps take about 0.3ms time and is not as fast as how it is in electrical synapses. Ca^{2+} ions start to go out from the cell gradually before the completion of action potential. Dopamine will be uptaken with postsynaptic neuron or reuptaked to the presynaptic neuron by DAT (Dopamine transporter). This modeling is the improved version of what Best et al. [7] did in 2009.

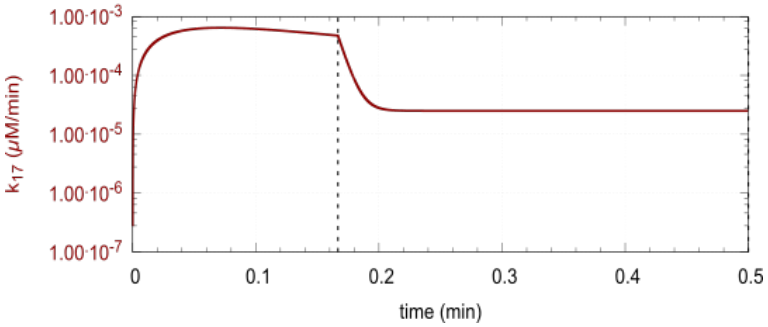

FIGURE 3.13: k_{17} flux as a function of time. Time scale is minute. After receiving action potential, k_{17} increase relative slowly (hysteretic effect) due to inflow of Ca2+to the cell. Before the end of action potential, k_{17} decreases in the result of Ca2+ release from the pumps.

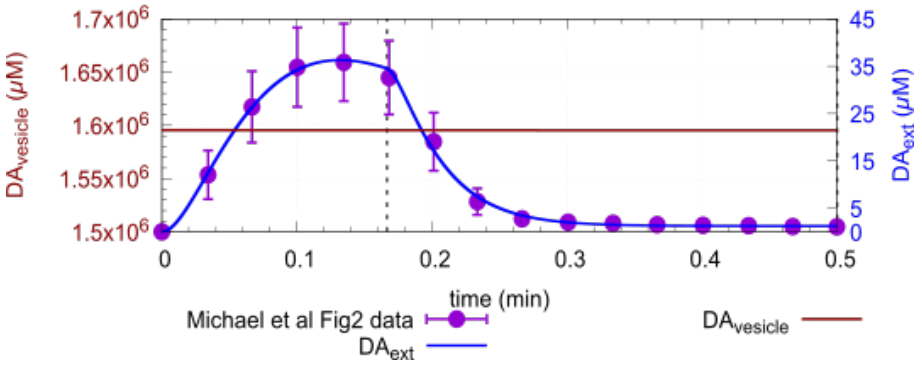

FIGURE 3.14: DA concentration in the synaptic cleft. Points are the experimentally determined DA concentrations. The concentration of DA in the synaptic cleft is related to the k_{17} flux. After receiving flux by the cell, Ca2+ ion concentration in the cell increase and trigger vesicle fusion to the presynaptic terminal membrane and release DA into the synaptic cleft. With withdrawal of Ca2+ ions from the calcium pumps in the membrane, DA concentration decrease in the synaptic cleft.

Chapter 4

Discussion

In this study, the main goal was to alter at least one parameter in each experiment and find how specific values of molecules affect the controlling system, involving dopamine in the nervous system.
Almost all the results show DOPA is a controlled variable tries to keep its levels near its set-point in presence of different perturbations. Dopamine is a species which helps DOPA maintain its set-point. However, more laboratory experiments are needed to show this specific features in this system experimentally. It can be a very noticeable fact in treating many dopamine related diseases.

A main condition to perform the robust controlling system and robustness of the DOPA homeostasis, is removing of controlling species (dopamine) by zero-order kinetics into the vesicle. The experimental results by Volz et al. [28] shows very low levels of K_M for VMAT-2 (0.289 μM), which supports this idea. Figures 3.1 to 3.3 illustrate how k_8 values affect DOPA, reaching its set-point. Transporter enzyme VMAT-2 is responsible enzyme to transfer dopamine to the presynaptic vesicles.

Sufficient amounts of compensatory flux (j_2) is very important in the function of the controlling system. When compensatory flux become close to zero, it is impossible to decrease the controlled variable (DA) to reduce the inhibition on the controlled variable , so the controller breaks down. This compensatory flux is based on controller motif 2 which is an inflow controller. It means that, in the loss of the controlled species due to enzymes or other environmental reasons, the controller tries to compensate this loss with an inflow flux by derepression. However, this controlling system does not perform very well when the controlled variable concentrations is more than its set-point. For example, Figure 3.11 shows that in higher levels of DOPA, DA values increase to down-regulate

the compensatory flux j_2, but it is not possible and the inflow controlling system is not helpful in this situation. This behaviour called integral windup [21].
Although it has been shown in Figure 1.3 that enzymes TH, DDC and VMAT2 form a channeling mechanism that prevents DA being free in the cytoplasm, high DA concentrations, may lead to more DA oxidation by ROS, MAO or Auto-oxidation. These reactions lead to cell toxicity and neuropsychiatric disorders [44]. Reactive oxygen species are related to many age-related diseases [45]. Also MAO activity may increase with age [46]. By influencing these oxidative molecules on DOPA, DA decrease to compensate for DOPA loss. Excess decease of DA may lead to movement disorder like PD or other age-related diseases.

Figure 3.14, nicely illustrates the sigmoidal curve of the relationship between external dopamine and time. The calculations suggest a hysteretic behaviour of releasing dopamine to the synaptic cleft by receiving action potential. Transporters, like other proteins, response the changes slightly and their status transition may take time. Decreasing external dopamine level may occur because of the presence of plasma membrane Ca2+- ATPase pumps. High levels of cellular calcium is toxic and leads to neuron apoptosis. Excess amount of calcium are pumped out from the cell by calcium pumps [47]. This function, lead to reduced amounts of calcium before the end of action potential, cause a decrease in external dopamine levels.However, Best et al. [7] suggest that DA reduction in external dopamine before the end of action potential, may occur due to low vesicular dopamine reservoir.

Our model results, fits the experimental results of external dopamine concentration, determined by in vivo voltammetry, after stimulation of rat dopaminergic cells done by Michael et al. [27].

Chapter 5

Conclusion and Outlook

The results suggest presence of a controlling system, with controlled variable DOPA and controller variable DA. To have the robust homeostasis for this controlling system, zero-order removal of controlled variable (DA) is required. Experimentally determined values of transporting DA to the synaptic vesicle shows $K_M = 0.289$ μM [28]. This result appear to be in favour of zero-order kinetics of DA removal and loading into the vesicle.

Results show that many factors are effective on performing the robust homeostasis of DOPA, which alter the concentration of DA in order to maintain DOPA at its set-point. This changes in DA concentration as controller variable, may cause different diseases like PD or addiction.

DA release into the synaptic cleft shows a hysteretic (time dependent) behaviour. This properties in DA release may be in relation to status changing of enzymes performing this process.

TH regulation by D2 Auto-receptors and re-entry of DA to cell by DAT, can be a subject of future closer observations. further studies needed to show the exact influence of different variables in the system, the relationship of Ca2+ ions and DA release into the synaptic cleft and influence and best amounts of medicinal DOPA (LDOPA) using to cure DA associated diseases

Bibliography

[1] Rune Kleppe, Qaiser Waheed, and Peter Ruoff. Dopa homeostasis by dopamine: A control-theoretic view. *International Journal of Molecular Sciences*, 22(23):12862, 2021.

[2] 2022. URL `http://www.scientificanimations.com/wiki-images`.

[3] URL `http://www.scientificanimations.com/wiki-images`.

[4] Peter Ruoff, Oleg Agafonov, Daniel Tveit, Kristian Thorsen, and Tormod Drengstig. Homeostatic controllers compensating for growth and perturbations. *PLOS ONE*, 14, 2019.

[5] *Principles of neural science*, volume 4. McGraw-hill New York, 4th edition, 2000.

[6] Shankar J Chinta and Julie K Andersen. Dopaminergic neurons. *The international journal of biochemistry & cell biology*, 37(5):942–946, 2005.

[7] Janet A Best, H Frederik Nijhout, and Michael C Reed. Homeostatic mechanisms in dopamine synthesis and release: a mathematical model. *Theoretical Biology and Medical Modelling*, 6(1):1–20, 2009.

[8] Patricia Muñoz, Sandro Huenchuguala, Irmgard Paris, and Juan Segura-Aguilar. Dopamine oxidation and autophagy. *Parkinson's disease*, 2012, 2012.

[9] Changliang Liu and Pascal S Kaeser. Mechanisms and regulation of dopamine release. *Current opinion in neurobiology*, 57:46–53, 2019.

[10] Anthony A Grace, Benjamin S Bunney, Holly Moore, and Christopher L Todd. Dopamine-cell depolarization block as a model for the therapeutic actions of antipsychotic drugs. *Trends in neurosciences*, 20(1):31–37, 1997.

[11] Gholson J Lyon, Anissa Abi-Dargham, Holly Moore, Jeffrey A Lieberman, Jonathan A Javitch, and David Sulzer. Presynaptic regulation of dopamine transmission in schizophrenia. *Schizophrenia bulletin*, 37(1):108–117, 2011.

[12] Rosaria Formisano, Katarzyna D Rosikon, Abhyudai Singh, and Harbinder S Dhillon. The dopamine membrane transporter plays an active modulatory role in synaptic dopamine homeostasis. *Journal of neuroscience research*, 2021.

[13] Kenneth L Davis, René S Kahn, Grant Ko, and Michae Davidson. Dopamine in schizophrenia: a review and reconceptualization. *The American journal of psychiatry*, 1991.

[14] Gail Tripp and Jeffery R Wickens. Neurobiology of adhd. *Neuropharmacology*, 57 (7-8):579–589, 2009.

[15] Roy A Wise and Mykel A Robble. *Dopamine and addiction*, volume 71. Annual review of psychology, 2020.

[16] Ming Chi Shih, Marcelo Queiroz Hoexter, Luiz Augusto Franco de Andrade, and Rodrigo Affonseca Bressan. Parkinson s disease and dopamine transporter neuroimaging: a critical review. *Sao Paulo Medical Journal*, 124(3):168–175, 2006.

[17] AHV Schapira, M Emre, P Jenner, and W Poewe. Levodopa in the treatment of parkinson's disease. *European Journal of Neurology*, 16(9):982–989, 2009.

[18] Walter B Cannon. *Organization for physiological homeostasis*, volume 9. Physiological reviews, 1929.

[19] Walter Bradford Cannon. Homeostasis. *The wisdom of the body. Norton, Newyork*, 1932.

[20] T Drengstig, IW Jolma, XY Ni, K Thorsen, XM Xu, and P Ruoff. A basic set of homeostatic controller motifs. *Biophysical journal*, 103(9):2000–2010, 2012.

[21] Jacqueline Wilkie, Michael A Johnson, and Reza Katebi. *Control engineering*. Macmillan International Higher Education, 2017.

[22] T Drengstig, XY Ni, K Thorsen, IW Jolma, and P Ruoff. Robust adaptation and homeostasis by autocatalysis. *The Journal of Physical Chemistry B*, 116(18): 5355–5363, 2012.

[23] Stephanie K Aoki, Gabriele Lillacci, Ankit Gupta, Armin Baumschlager, David Schweingruber, and Mustafa Khammash. A universal biomolecular integral feedback controller for robust perfect adaptation. *Nature*, 570(7762):533–537, 2019.

[24] Kristian Thorsen, Peter Ruoff, and Tormod Drengstig. Control theoretic properties of physiological controller motifs. In *2013 International Conference on System Science and Engineering (ICSSE)*, pages 165–170. IEEE, 2013.

[25] Kenneth E Neet and G Robert Ainslie Jr. *Methods in enzymology*. Elsevier, 1980.

[26] Carl Frieden. *Slow transitions and hysteretic behavior in enzymes*, volume 48. Annual Reviews 4139 El Camino Way, PO Box 10139, Palo Alto, CA 94303-0139, USA, 1979.

[27] Adrian C Michael, Masato Ikeda, and Joseph B Justice Jr. Mechanisms contributing to the recovery of striatal releasable dopamine following mfb stimulation. *Brain research*, 421(1-2):325–335, 1987.

[28] Trent J Volz, Glen R Hanson, and Annette E Fleckenstein. Measurement of kinetically resolved vesicular dopamine uptake and efflux using rotating disk electrode voltammetry. *Journal of neuroscience methods*, 155(1):109–115, 2006.

[29] Shamima Nasrin, Hiroshi Ichinose, Hiroyoshi Hidaka, and Toshiharu Nagatsu. Recombinant human tyrosine hydroxylase types 1–4 show regulatory kinetic properties for the natural (6 r)-tetrahydrobiopterin cofactor. *The Journal of Biochemistry*, 116 (2):393–398, 1994.

[30] Mitchell A Lazar, Alexandre J Lockfeld, Roger JW Truscott, and Jack D Barchas. Tyrosine hydroxylase from bovine striatum: catalytic properties of the phosphorylated and nonphosphorylated forms of the purified enzyme. *Journal of Neurochemistry*, 39(2):409–422, 1982.

[31] María Teresa Bueno-Carrasco, Jorge Cuéllar, Marte I Flydal, César Santiago, Trond-André Kråkenes, Rune Kleppe, José R López-Blanco, Miguel Marcilla, Knut Teigen, Sara Alvira, et al. Structural mechanism for tyrosine hydroxylase inhibition by dopamine and reactivation by ser40 phosphorylation. *Nature communications*, 13(1):1–16, 2022.

[32] Giri R Sura, S Colette Daubner, and Paul F Fitzpatrick. Effects of phosphorylation by protein kinase a on binding of catecholamines to the human tyrosine hydroxylase isoforms. *Journal of neurochemistry*, 90(4):970–978, 2004.

[33] Mariarita Bertoldi. Mammalian dopa decarboxylase: structure, catalytic activity and inhibition. *Archives of biochemistry and biophysics*, 546:1–7, 2014.

[34] Teresa M Olefirowicz and Andrew G Ewing. Dopamine concentration in the cytoplasmic compartment of single neurons determined by capillary electrophoresis. *Journal of neuroscience methods*, 34(1-3):11–15, 1990.

[35] Jennifer B Chien, Ross A Wallingford, and Andrew G Ewing. Estimation of free dopamine in the cytoplasm of the giant dopamine cell of planorbis corneus by voltammetry and capillary electrophoresis. *Journal of neurochemistry*, 54(2):633–638, 1990.

[36] Jean-Sébastien Schonn, Claire Desnos, Jean-Pierre Henry, and François Darchen. Transmitter uptake and release in pc12 cells overexpressing plasma membrane monoamine transporters. *Journal of neurochemistry*, 84(4):669–677, 2003.

[37] Stefano Fogal, Marcello Carotti, Laura Giaretta, Federico Lanciai, Leonardo Nogara, Luigi Bubacco, and Elisabetta Bergantino. Human tyrosinase produced in insect cells: a landmark for the screening of new drugs addressing its activity. *Molecular biotechnology*, 57(1):45–57, 2015.

[38] Hong-Yan Han, Jae-Rin Lee, Wei-An Xu, Myong-Joon Hahn, Jun-Mo Yang, and Yong-Doo Park. Effect of cl- on tyrosinase: complex inhibition kinetics and biochemical implication. *Journal of Biomolecular Structure and Dynamics*, 25(2):165–171, 2007.

[39] Jan Haavik. L-dopa is a substrate for tyrosine hydroxylase. *Journal of neurochemistry*, 69(4):1720–1728, 1997.

[40] Yvonne Schmitz, Marianne Benoit-Marand, François Gonon, and David Sulzer. Presynaptic regulation of dopaminergic neurotransmission. *Journal of neurochemistry*, 87(2):273–289, 2003.

[41] Min Li, Frantisek Hubálek, Paige Newton-Vinson, and Dale E Edmondson. High-level expression of human liver monoamine oxidase a in pichia pastoris: comparison with the enzyme expressed in saccharomyces cerevisiae. *Protein expression and purification*, 24(1):152–162, 2002.

[42] Joanne Ng, Apostolos Papandreou, Simon J Heales, and Manju A Kurian. Monoamine neurotransmitter disorders—clinical advances and future perspectives. *Nature Reviews Neurology*, 11(10):567–584, 2015.

[43] Torbjoern G Nygaard, CD Marsden, and RC Duvoisin. Dopa-responsive dystonia. *Advances in neurology*, 50:377–384, 1988.

[44] Vignayanandam R Muddapu, Karthik Vijayakumar, Keerthiga Ramakrishnan, and V Srinivasa Chakravarthy. A computational model of levodopa-induced toxicity in substantia nigra pars compacta in parkinson's disease. *arXiv preprint arXiv:2004.08320*, 2020.

[45] Ilaria Liguori, Gennaro Russo, Francesco Curcio, Giulia Bulli, Luisa Aran, David Della-Morte, Gaetano Gargiulo, Gianluca Testa, Francesco Cacciatore, Domenico Bonaduce, et al. Oxidative stress, aging, and diseases. *Clinical interventions in aging*, 13:757, 2018.

[46] IA Volchegorskii, SE Shemyakov, VV Turygin, and NV Malinovskaya. The age dynamics of monoamine oxidase activity and levels of lipid peroxidation products in the human brain. *Neuroscience and behavioral physiology*, 34(4):303–305, 2004.

[47] Asma Zaidi, Mercy Adewale, Lauren McLean, and Paul Ramlow. The plasma membrane calcium pumps—the old and the new. *Neuroscience letters*, 663, 2018.